Supplementary Material (ESI) for Journal of Materials Chemistry
This journal is (c) The Royal Society of Chemistry 2009

Effects of size, capping agent, and concentration of CdSe and CdTe quantum dots doped into a nematic liquid crystal on the optical and electro-optic properties of the final colloidal liquid crystal mixture

Brandy Kinkead and Torsten Hegmann*

Department of Chemistry, University of Manitoba, 144 Dysart Road, Winnipeg, Manitoba, Canada.
Fax: 1 204 474 7608; Tel: 1 204 474 7535; E-mail: hegmannt@cc.umanitoba.ca

Electronic Supplementary Information (ESI)

Contents Page(s)

1. K_{11} elastic constants for all mixtures

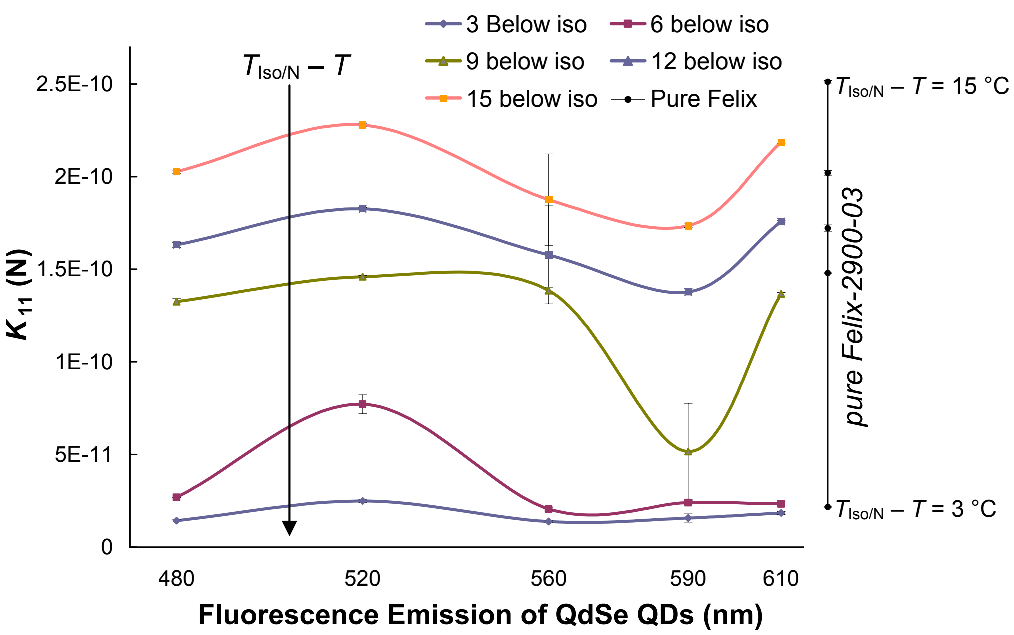

Fig. S1 Plots of the K_{11} elastic constant versus QD size (shown as fluorescence emission wavelength maximum of the CdSe QDs) at different reduced temperatures ($T_{Iso/N} - T$ = 15 °C top to $T_{Iso/N} - T$ = 3 °C bottom) for the 2 wt% mixtures. The values for pure **LC1** at the same reduced temperatures are shown on the right for comparison (black series).

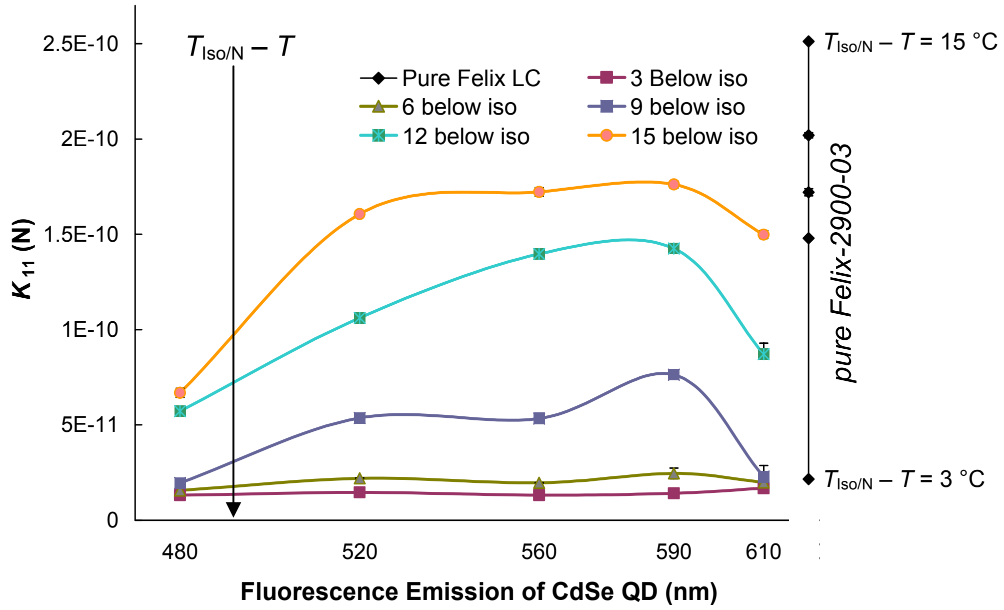

Fig. S2 Plots of the K_{11} elastic constant versus QD size (shown as fluorescence emission wavelength maximum of the CdSe QDs) at different reduced temperatures ($T_{Iso/N} - T$ = 15 °C top to $T_{Iso/N} - T$ = 3 °C bottom) for the 5 wt% mixtures. The values for pure **LC1** at the same reduced temperatures are shown on the right for comparison (black series).

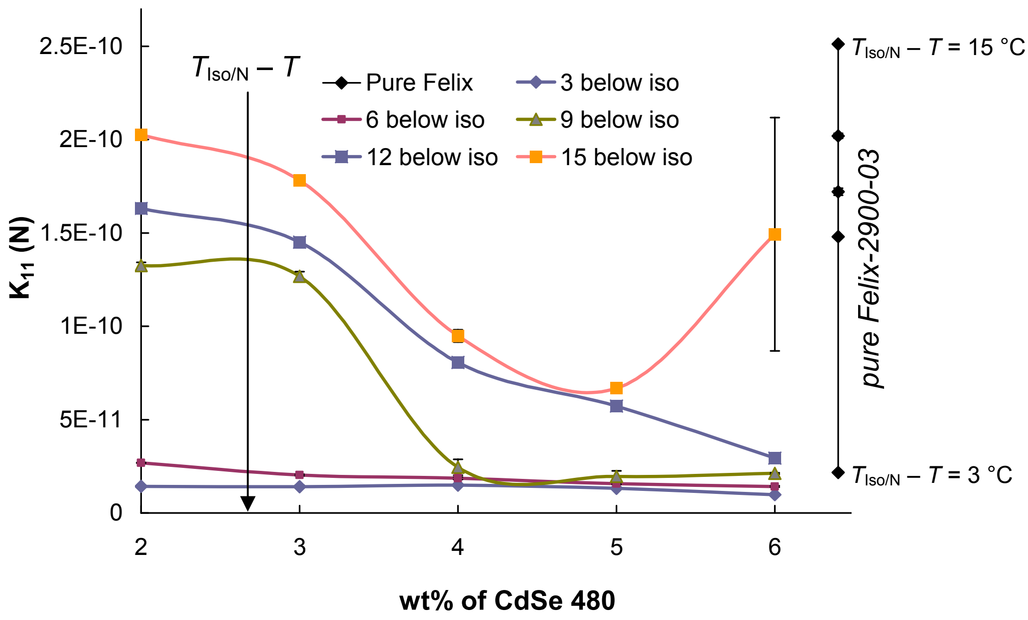

Fig. S3 Plots of the K_{11} elastic constant versus wt% of the $CdSe_{480}$ QDs at different reduced temperatures ($T_{Iso/N} - T$ = 15 °C top to $T_{Iso/N} - T$ = 3 °C bottom). Values for pure **LC1** at the same reduced temperatures are shown on the right for comparison (black series).

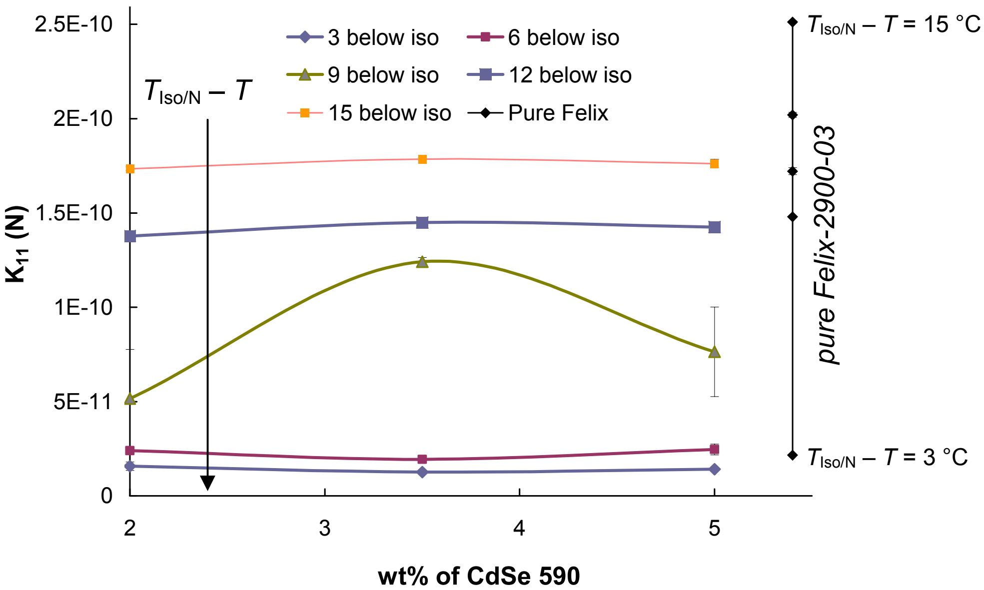

Fig. S4 Plots of the K_{11} elastic constant versus wt% of the $CdSe_{590}$ QDs at different reduced temperatures ($T_{Iso/N} - T$ = 15 °C top to $T_{Iso/N} - T$ = 3 °C bottom). Values for pure **LC1** at the same reduced temperatures are shown on the right for comparison (black series).

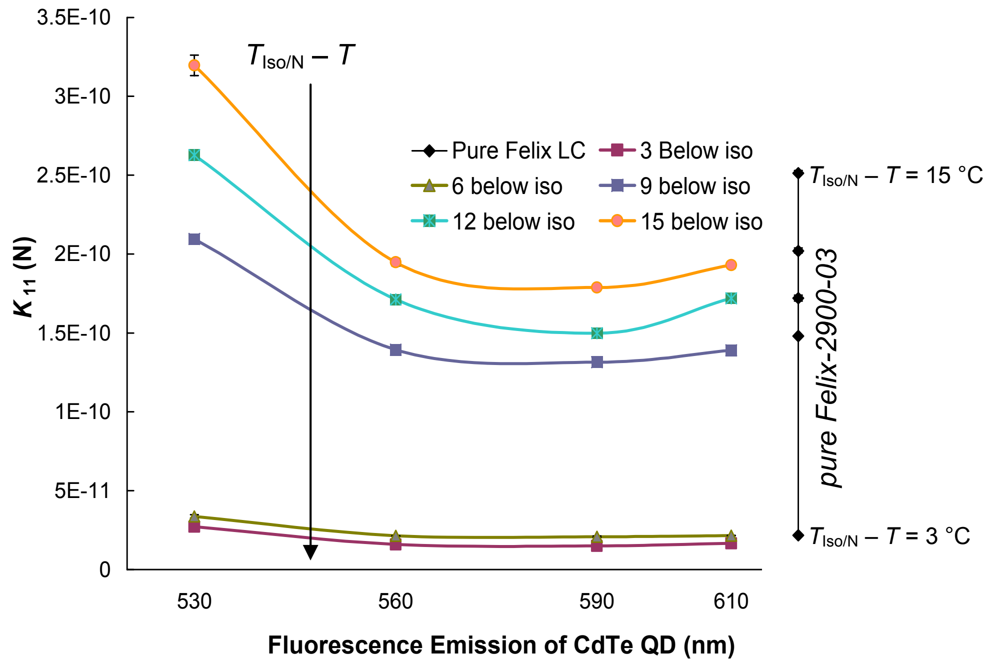

Fig. S5 Plots of the K_{11} elastic constant versus QD size (shown as fluorescence emission wavelength maximum of the CdTe QDs) at different reduced temperatures ($T_{Iso/N} - T$ = 15 °C top to $T_{Iso/N} - T$ = 3 °C bottom) for the 2 wt% mixtures. The values for pure **LC1** at the same reduced temperatures are shown on the right for comparison (black series).

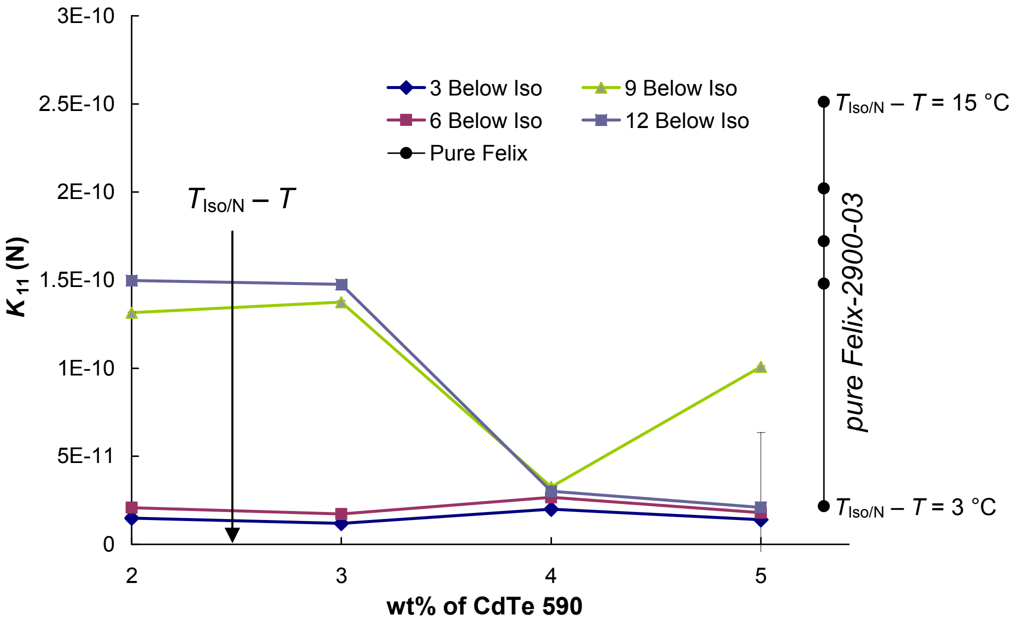

Fig. S6 Plots of the K_{11} elastic constant versus wt% of the $CdTe_{590}$ QDs at different reduced temperatures ($T_{Iso/N} - T = 15$ °C top to $T_{Iso/N} - T = 3$ °C bottom). Values for pure **LC1** at the same reduced temperatures are shown on the right for comparison (black series).

2. Inhomogeneous alignment (switching) of LC1 doped with 1 wt% $CdSe_{480}$

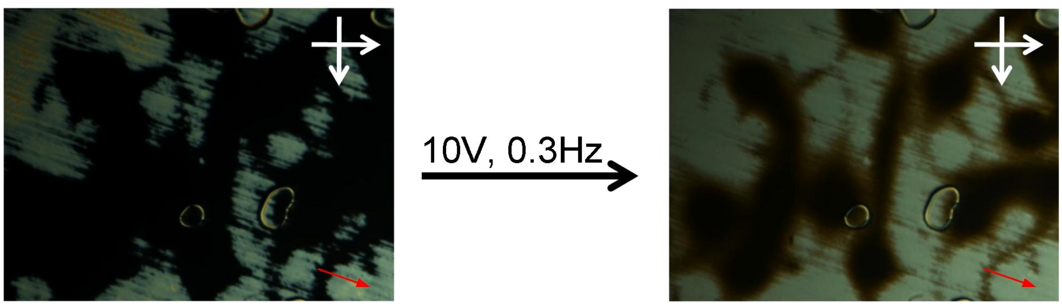

Fig. S7 Optical photomicrographs of the 1 wt% $CdSe_{480}$ in **LC1** mixture with (right) and without (left) an applied field. Red arrows show the rubbing direction of the cell.

3. Resistivity, *R*, of all QD-doped LC1 mixtures*

	Resistivity, R in Ω (SD = standard deviation)									
	3 °C below Iso		6 °C below Iso		9 °C below Iso		12 °C below Iso		15 °C below Iso	
Sample Description	Value	SD	Value	SD	Value	SD	Value	SD	Value	SD
pure Felix-2900-03	10.41E+10	3.19E+09	16.9E+10	3.07E+09	21.5E+10	2.61E+10	23.2E+10	5.94E+09	27.6E+10	1.38E+10
2.0% $CdSe_{480}$	3.187E+10	5.21E+08	3.89E+10	2.44E+08	4.58E+10	2.48E+08	5.30E+10	3.49E+08	6.08E+10	1.99E+08
2.0% $CdSe_{520}$	2.924E+10	2.01E+08	3.44E+10	3.84E+08	4.10E+10	7.09E+08	4.75E+10	2.18E+08	5.44E+10	1.28E+09
2.0% $CdSe_{560}$	2.227E+10	4.85E+08	2.76E+10	2.76E+08	3.19E+10	3.71E+08	5.38E+10	4.05E+08	6.25E+10	2.88E+08
2.0% $CdSe_{590}$	2.983E+10	1.71E+08	3.51E+10	4.74E+08	4.07E+10	3.28E+08	4.71E+10	4.64E+08	5.30E+10	8.16E+08
2.0% $CdSe_{610}$	2.785E+10	2.47E+08	3.29E+10	1.82E+08	3.75E+10	2.99E+08	4.13E+10	3.64E+08	4.73E+10	2.13E+08
5.0% $CdSe_{480}$	2.748E+10	3.73E+08	3.26E+10	5.17E+08	3.87E+10	4.85E+08	4.46E+10	6.50E+08	5.03E+10	7.08E+08
5.0% $CdSe_{520}$	2.678E+10	1.09E+08	3.27E+10	2.36E+08	3.88E+10	2.89E+08	4.63E+10	8.36E+08	5.53E+10	1.09E+09
5.0% $CdSe_{560}$	2.878E+10	5.58E+08	3.53E+10	4.28E+08	4.35E+10	1.37E+09	4.96E+10	4.28E+08	5.78E+10	2.27E+08
5.0% $CdSe_{590}$	2.22E+10	9.68E+08	3.15E+10	5.40E+08	3.76E+10	2.87E+08	4.35E+10	9.54E+08	5.14E+10	3.61E+08
5.0% $CdSe_{610}$	2.613E+10	4.43E+08	3.39E+10	3.71E+08	4.44E+10	3.77E+08	5.62E+10	6.72E+08	7.05E+10	2.75E+08
2.0% $CdTe_{530}$	1.35E+10	2.14E+08	1.48E+10	2.13E+08	1.60E+10	5.50E+08	1.71E+10	1.25E+08	1.93E+10	3.41E+08
2.0% $CdTe_{560}$	0.51E+10	5.63E+07	0.63E+10	0.00E+00	0.75E+10	6.31E+07	0.87E+10	1.59E+08	1.01E+10	4.85E+07
2.0% $CdTe_{590}$	1.79E+10	6.00E+07	2.20E+10	1.35E+08	2.65E+10	4.79E+07	3.04E+10	2.23E+08	3.51E+10	1.25E+08
2.0% $CdTe_{610}$	0.63E+10	4.19E+07	0.78E+10	1.07E+06	0.93E+10	1.83E+08	1.09E+10	1.59E+07	1.25E+10	4.29E+07
3.0% $CdSe_{480}$	2.71E+10	6.92E+08	3.21E+10	1.81E+08	3.70E+10	2.12E+08	4.28E+10	2.06E+08	4.83E+10	2.31E+08
4.0% $CdSe_{480}$	2.198E+10	1.56E+08	2.69E+10	2.46E+08	3.16E+10	1.65E+08	3.56E+10	1.13E+08	4.03E+10	2.11E+08
6.0% $CdSe_{480}$	2.50E+10	3.21E+08	3.03E+10	5.30E+08	3.60E+10	2.78E+08	4.06E+10	6.16E+08	4.62E+10	7.02E+08
3.5% $CdSe_{590}$	2.34E+10	6.84E+07	2.74E+10	2.48E+08	3.13E+10	1.11E+08	3.29E+10	4.62E+07	3.67E+10	1.54E+08
3.0% $CdTe_{590}$	0.26E+10	1.83E+07	0.31E+10	1.22E+07	0.36E+10	0.00E+00	0.43E+10	2.28E+07	—	—
4.0% $CdTe_{590}$	0.27E+10	1.30E+07	0.32E+10	5.24E+07	0.36E+10	1.44E+07	0.43E+10	5.33E+07	—	—
5.0% $CdTe_{590}$	0.27E+10	3.23E+07	0.33E+10	1.19E+07	0.42E+10	1.93E+07	0.525E+10	3.65E+07	—	—

*Note, all resistivity values are on the order of GΩ (10^9 Ω) and larger.

4. Enlarged POM images

Below, enlarged POM images of all mixtures are provided allowing for a better assessment of alignment effects caused by the CdSe and CdTe QDs, and to better visualize the aggregation tendencies of some QDs in **LC1** at certain concentrations (see Figures S8 to S14).

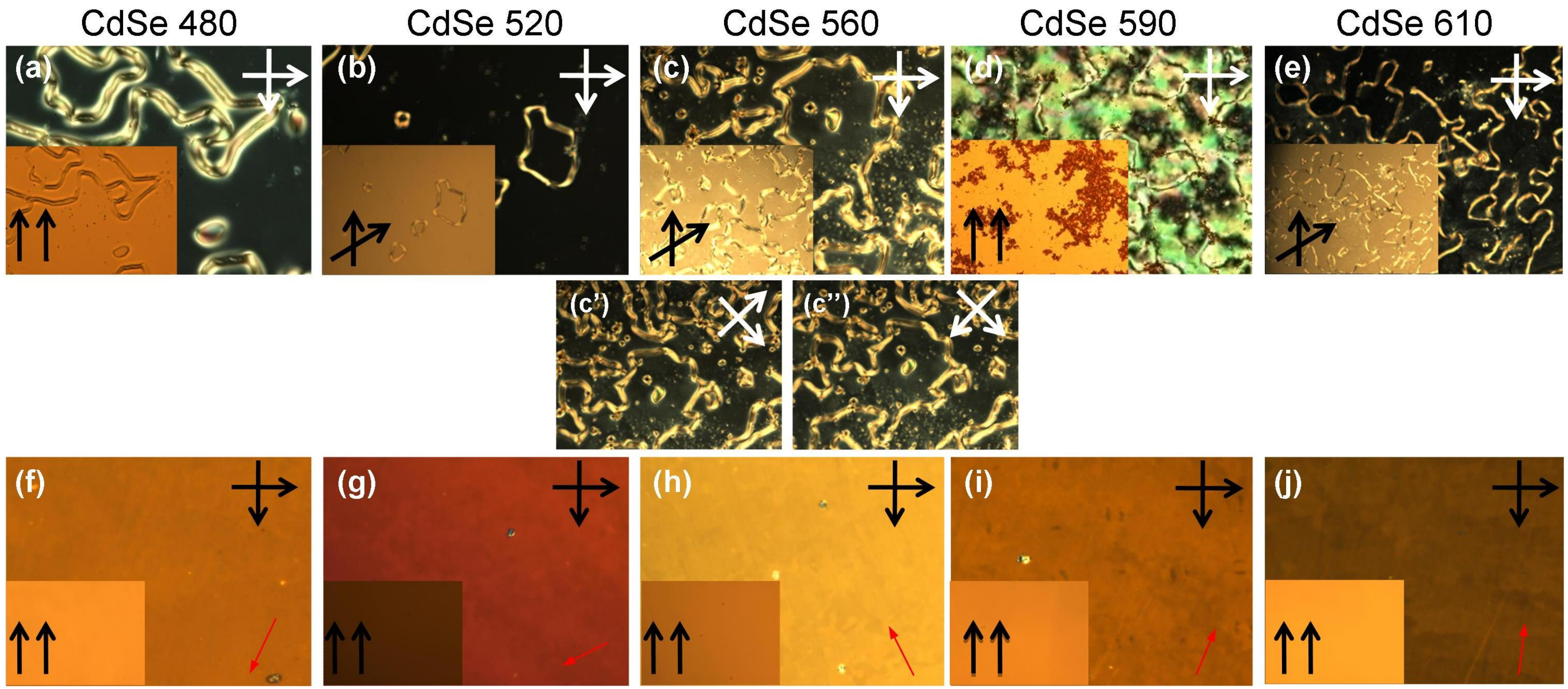

Fig. S8 (see Figure 3 in main text): POM images of the 2 wt% mixtures of $CdSe_{480}$-$CdSe_{610}$ in the nematic phase of **LC1** at $T_{Iso/N} - T = 9$ °C between plain glass slides (a-e) and in planar aligned cells (f-j). Images (c') and (c'') show the thin film of (c) after sample rotation between crossed polarizers 45° to the left and 45° to the right (evidencing vertical alignment of the dark domains). Red arrows show rubbing direction of the planar cells. The insert in each figure shows the same area with parallel (un-crossed) or slightly un-crossed polarizers.

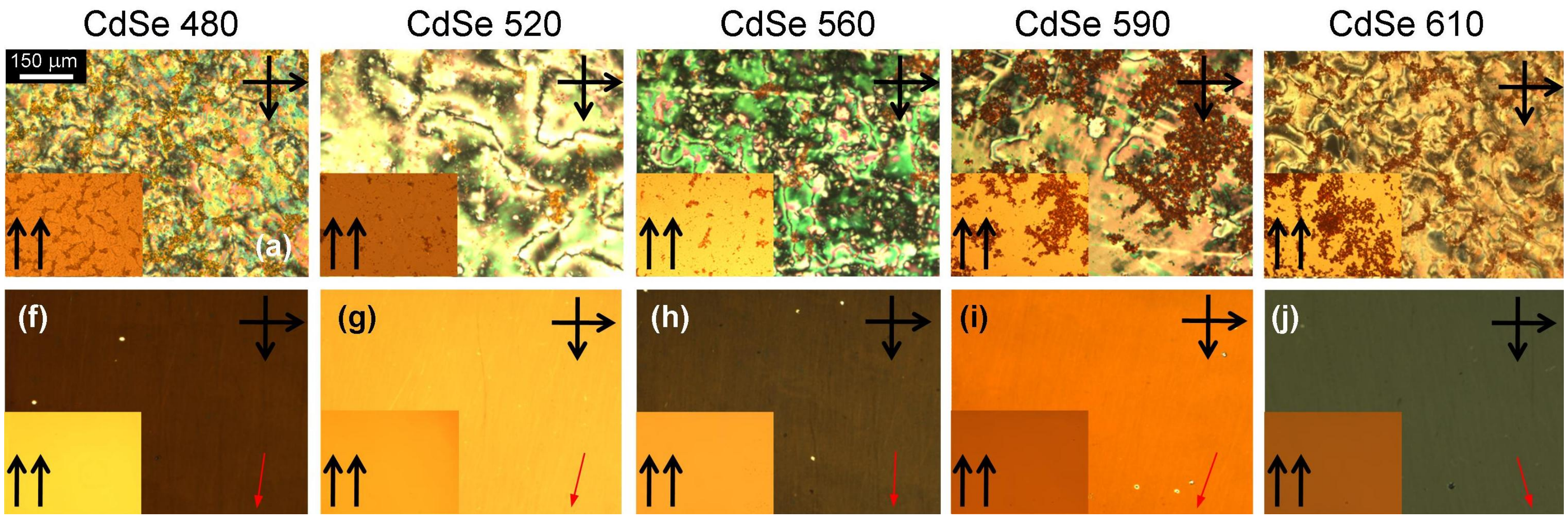

Fig. S9 (see Figure 5 in main text): POM images of the 5 wt% mixtures of $CdSe_{480}$-$CdSe_{610}$ QDs in the nematic phase of **LC1** at $T_{Iso/N} - T = 9$ °C between plain glass slides (a-e) and in planar aligned cells (f-j). Red arrows show rubbing direction of the planar cells. The insert in each figure shows the same area with parallel (un-crossed) polarizers.

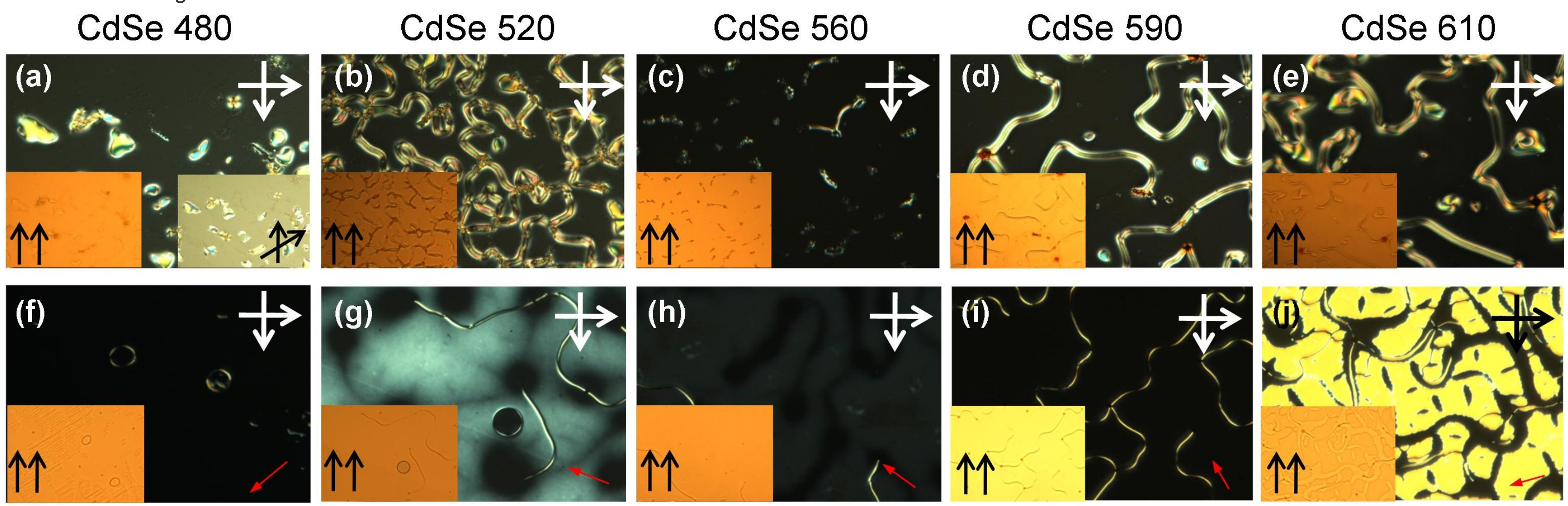

Fig. S10 (see Figure 11 in main text): POM images of the 1 wt% mixtures of $CdSe_{480}$-$CdSe_{610}$ QDs in the nematic phase of **LC1** at $T_{Iso/N} - T = 9$ °C between plain glass slides (a-e) and in planar aligned cells (f-j). Red arrows show rubbing direction of the planar cells. The left insert in figures (a-j) shows the same sample area with parallel (un-crossed) polarizers and the insert in figure (a) with slightly un-crossed polarizers (~30°).

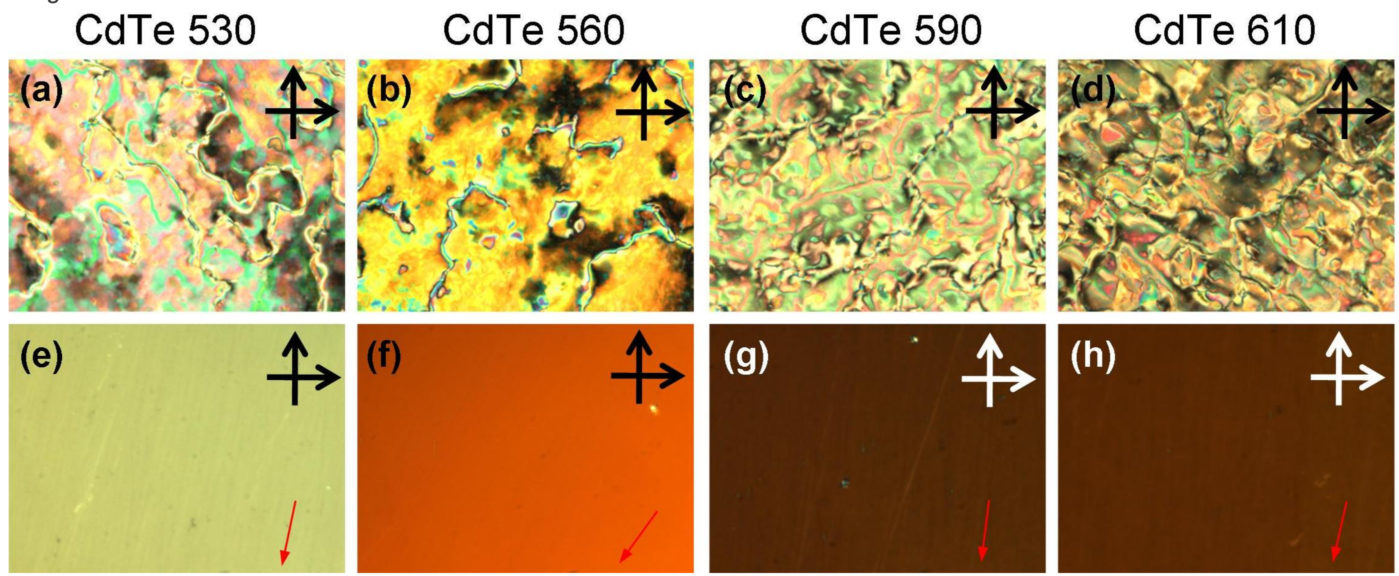

Fig. S11 (see Figure 12 in main text): POM images of the 2 wt% mixtures of the $CdTe_{530}$-$CdTe_{610}$ QDs in the nematic phase of **LC1** at $T_{Iso/N} - T = 9$ °C between plain glass slides (a-d) and planar aligned cells (e-h). Red arrows show rubbing direction of the planar cells.

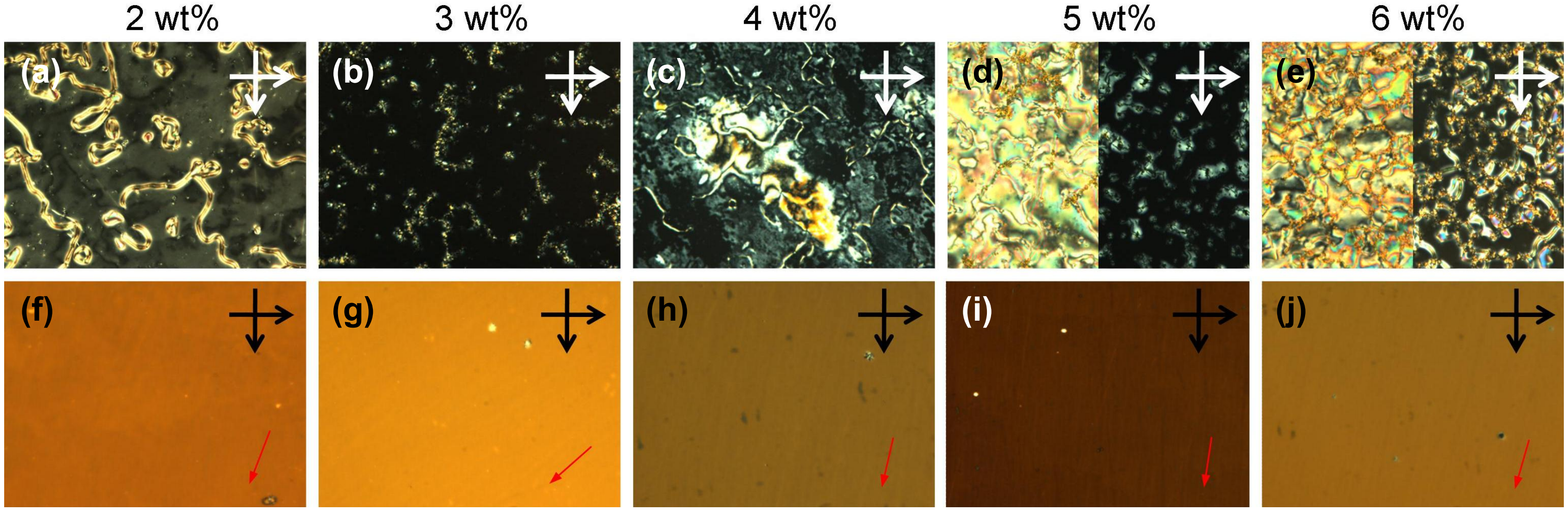

Fig. S12 POM images of the different concentrations of the $CdSe_{480}$ QDs in the nematic phase of **LC1** at $T_{Iso/N} - T = 9$ °C between plain glass slides (a) at 2 wt%, (b) at 3 wt%, (c) at 4 wt%, (d) at 5 wt%, (e) at 6 wt% and in planar aligned cells (f) at 2 wt%, (g) at 3 wt%, (h) at 4 wt%, (i) at 5 wt%, (j) at 6 wt%. Red arrows show rubbing direction of the planar cells. At 5 and 6 wt% between plain, untreated glass slides, areas (domains) with planar alignment and evidence of $CdSe_{480}$ QD aggregation as well as homeotropically aligned domains coexist [images of both domains are shown; see images (d) and (e)].

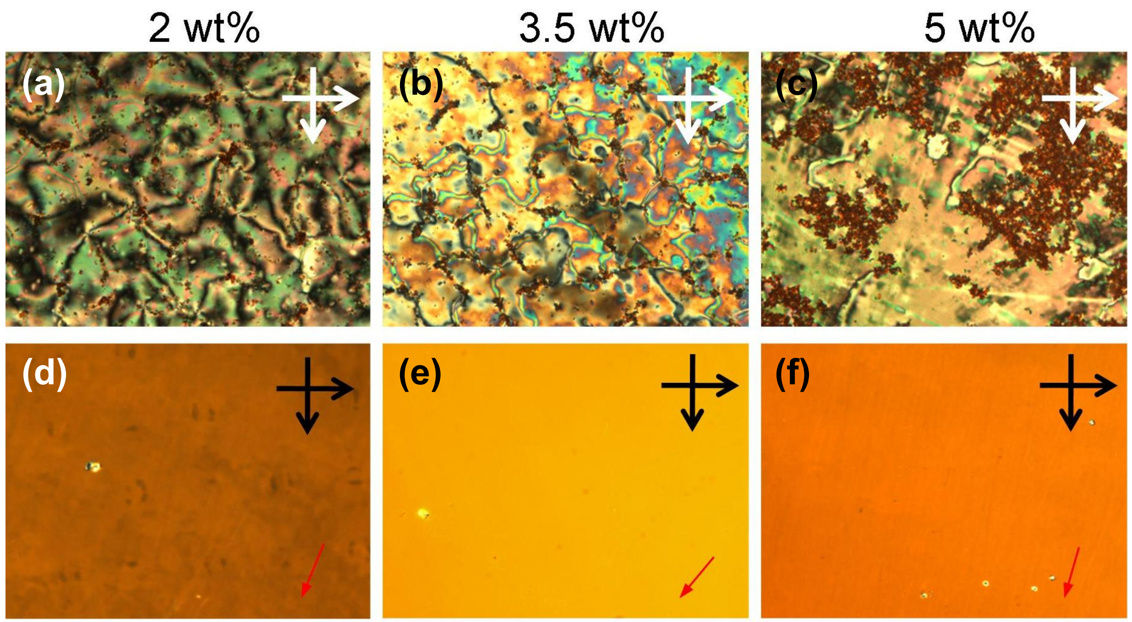

Fig. S13 POM images of the different concentrations of the $CdSe_{590}$ QDs in the nematic phase of **LC1** at $T_{Iso/N} - T = 9$ °C between plain glass slides (a) at 2 wt%, (b) at 3.5 wt%, (c) at 5 wt% and in planar aligned cells (d) at 2 wt%, (e) at 3.5 wt%, (f) at 5 wt%. Red arrows show rubbing direction of the planar cells.

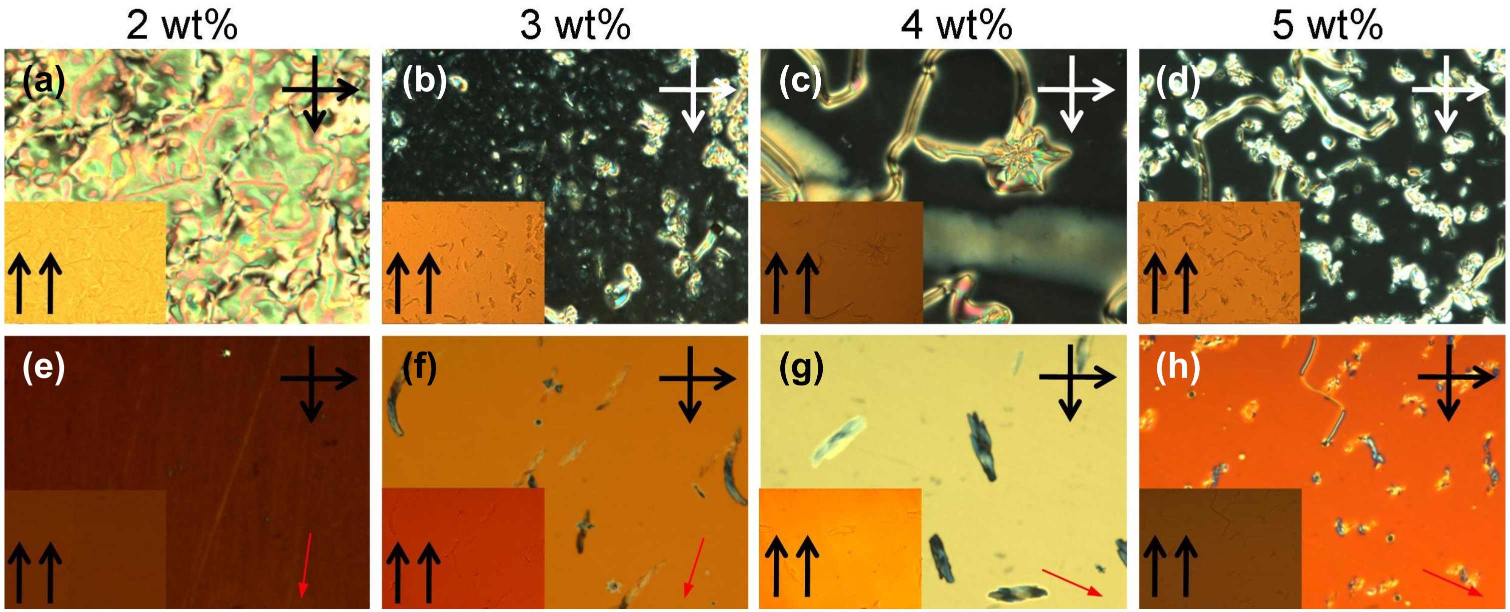

Fig. S14 POM images of the different concentrations of the $CdTe_{590}$ QDs in the nematic phase of **LC1** at $T_{Iso/N} - T = 9$ °C between plain glass slides (a) at 2 wt%, (b) at 3 wt%, (c) at 4 wt%, (d) at 5 wt% and in planar aligned cells (e) at 2 wt%, (f) at 3 wt%, (g) at 4 wt%, (h) at 5 wt%. Red arrows show rubbing direction of the planar cells. The insert in each figure shows the same area with parallel (un-crossed) polarizers.

Supplementary Material (ESI) for Journal of Materials Chemistry
This journal is (c) The Royal Society of Chemistry 2009

5. UV-vis spectra of TGA-capped CdTe QDs

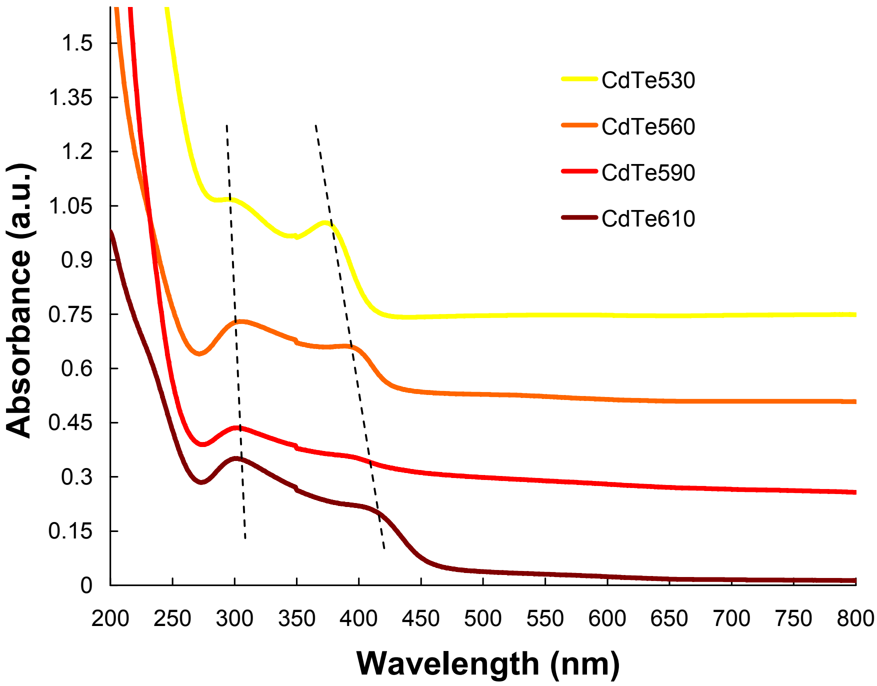

Fig. S15 UV-vis spectra of thioglycolic acid-capped CdTe QDs in water.

6. TEM analysis of TGA-capped CdTe QDs before size separation

High-resolution transmission electron microscopy (TEM) images were obtained on a Jeol ultrahigh resolution FEG-T/STEM operating at an acceleration voltage of 200 kV. A 10 µL drop of the QD solution prior to size separation was drop-cast on a carbon-coated copper grid (400-mesh) and dried for at least 1 hour.

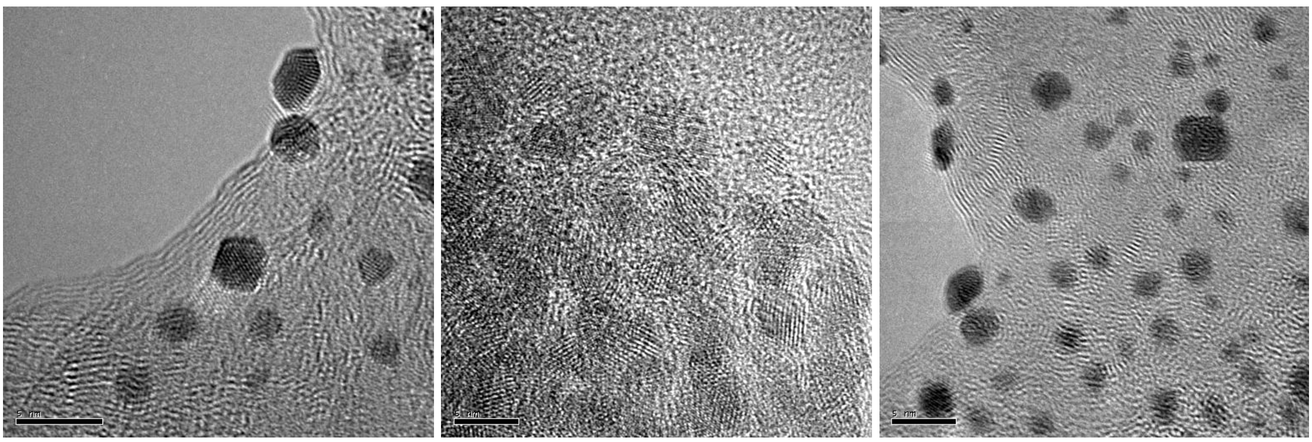

Fig. S16 High-resolution TEM image of thioglycolic-capped CdTe QDs before size separation (scale bar in each image = 5 nm).

Figure S16 shows the high-resolution TEM images of the thioglycolic acid-capped CdTe QDs before size separation as described in reference [69] in the main text. The TEM images clearly show that the sizes range from ca. 2.5 to 5.0 nm. For most of the QD homogeneous crystalline domains with cubic zinc blende crystal structure, which is commonly observed for CdTe QDs capped with thioglycolic acid in this size regime (see for example: S. K. Pradhan, Z. T. Deng, F. Tang, C. Wang, Y. Ren, P. Moeck, V. Petkov, *J. Appl. Phys.*, 2007, **102**, 044304). Thereafter, we have used the photoluminescence and UV-vis absorption spectra to determine the size and size distribution using photoluminescence and excitonic absorption peak maxima and FWHM of the emission peaks, which provide equivalents of fingerprints for the QD size. This method provides more precise bulk information on QD size and size distribution in comparison to often problematic and software-dependent TEM image analysis tools.